Manganese superoxide dismutase expression in endothelial progenitor cells accelerates wound healing in diabetic mice

Eric J. Marrotte,[1] Dan-Dan Chen,[1,2] Jeffrey S. Hakim,[1] and Alex F. Chen[1,2,3]

[1]Department of Surgery, Vascular Medicine Institute, McGowan Institute of Regenerative Medicine, University of Pittsburgh School of Medicine, Pittsburgh, Pennsylvania, USA. [2]Vascular Surgery Research, Veterans Affairs Pittsburgh Healthcare System, Pittsburgh, Pennsylvania, USA. [3]The Second Military Medical University, Shanghai, China.

Amputation as a result of impaired wound healing is a serious complication of diabetes. Inadequate angiogenesis contributes to poor wound healing in diabetic patients. Endothelial progenitor cells (EPCs) normally augment angiogenesis and wound repair but are functionally impaired in diabetics. Here we report that decreased expression of manganese superoxide dismutase (MnSOD) in EPCs contributes to impaired would healing in a mouse model of type 2 diabetes. A decreased frequency of circulating EPCs was detected in type 2 diabetic (*db/db*) mice, and when isolated, these cells exhibited decreased expression and activity of MnSOD. Wound healing and angiogenesis were markedly delayed in diabetic mice compared with normal controls. For cell therapy, topical transplantation of EPCs onto excisional wounds in diabetic mice demonstrated that diabetic EPCs were less effective than normal EPCs at accelerating wound closure. Transplantation of diabetic EPCs after *MnSOD* gene therapy restored their ability to mediate angiogenesis and wound repair. Conversely, siRNA-mediated knockdown of MnSOD in normal EPCs reduced their activity in diabetic wound healing assays. Increasing the number of transplanted diabetic EPCs also improved the rate of wound closure. Our findings demonstrate that cell therapy using diabetic EPCs after ex vivo MnSOD gene transfer accelerates their ability to heal wounds in a mouse model of type 2 diabetes.

Introduction

According to the Center for Disease Control and Prevention, refractory wounds lead to over 72,000 amputations each year in diabetic patients despite of advances in wound care (1). Vascular complications in diabetic patients, such as impaired angiogenesis, contribute to poor blood flow at the wound site, impeding the optimal endogenous regenerative response (2). Efficacious treatments are being explored to overcome poor angiogenesis in diabetic wound. Endothelial progenitor cells (EPCs), a key cell type involved in angiogenesis, can migrate to the injury/ischemia site and play an important role in vascular maintenance and angiogenesis, which raises interest in their implications in wound healing (3, 4). However, ample studies indicate that EPCs are dysfunctional in diabetic patients. These studies show that the number of circulating EPCs is significantly reduced in type 1 and type 2 diabetic patients (5, 6). Ex vivo functions of EPCs, including migration, adhesion, and tube formation, are also impaired in diabetes (7–9). Compelling evidence indicates that EPC dysfunction represents a mechanism for impaired angiogenesis and subsequent poor wound healing in diabetes (5–11). However, the mechanisms underlying EPC dysfunction in diabetes are still poorly understood.

Ex vivo evidence and in vivo evidence indicate that hyperglycemia and advanced glycoxidation products contribute to impaired wound healing in diabetes (12). Hyperglycemia is a hallmark of diabetes and leads to increased ROS and cellular damage (13, 14). We have demonstrated that hyperglycemia augments the superoxide anion generation in skin tissue by activating NADPH oxidase and protein kinase C, resulting in delayed wound healing in diabetic mice (15). Accumulation of ROS leads to widespread cellular damage and poor wound neovascularization (16). Normal EPCs have been shown to express intrinsically high levels of the antioxidant enzyme manganese superoxide dismutase (MnSOD), which plays a key role in EPC resistance to oxidative stress via scavenging mitochondrial ROS (mtROS) (17–19). Recent studies have shown that high glucose elevates oxidative stress and decreases EPC survival by inhibiting cell proliferation, NO production, MMP-9 activity, and migration (20, 21). These observations indicate that a loss of tolerance to hyperglycemia-induced excessive oxidative stress in EPCs may lead to their dysfunction in diabetes. Further characterization and better understanding of the mechanisms underlying impaired ROS resistance in diabetic EPCs could provide a basis for therapeutic application of EPCs in diabetic wound healing.

Based on the aforementioned studies, we tested the hypothesis that decreased MnSOD in EPCs may be a critical contributor to impaired EPC angiogenesis in type 2 diabetic wound repair. We isolated EPCs from the type 2 *db/db* diabetic mice and studied their functions both ex vivo and in vivo. Our results demonstrate that diabetic EPCs exhibit decreased MnSOD expression and enzymatic activity and develop elevated levels of oxidative stress. Ex vivo gene therapy of *MnSOD* for diabetic EPCs prior to their transplantation onto diabetic wound restored their angiogenic functions in vivo, resulting in accelerated wound repair. Finally, we provide evidence that both the number and functions of transplanted EPCs play significant roles in their regenerative capacity during wound healing, which should be taken into considerations when developing EPC-based cell therapies clinically.

Authorship note: Eric J. Marrotte and Dan-Dan Chen are co–first authors.

Conflict of interest: The authors have declared that no conflict of interest exists.

Citation for this article: *J Clin Invest.* 2010;120(12):4207–4219. doi:10.1172/JCI36858.

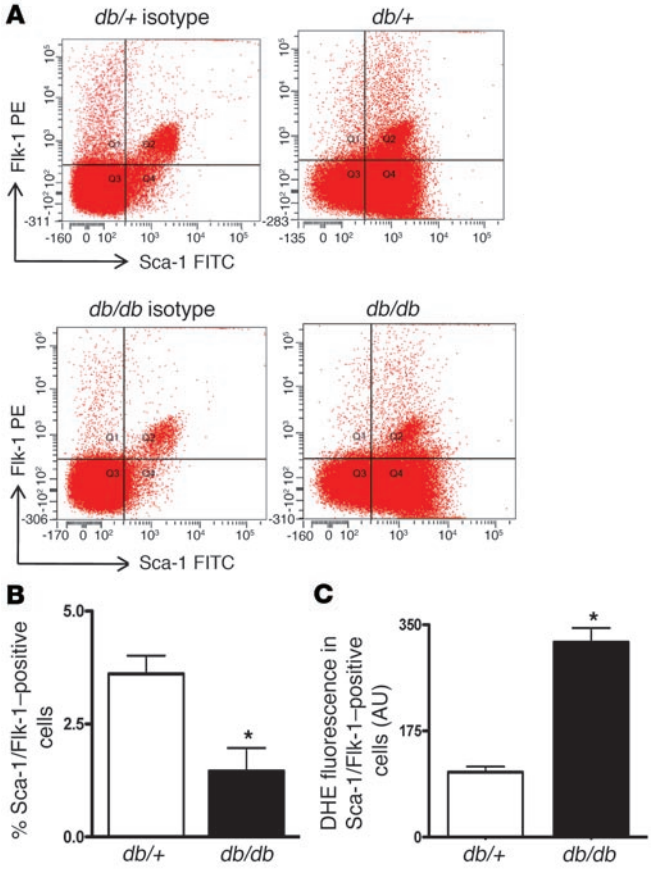

Figure 1
Flow cytometry analysis of mouse circulating EPCs. (**A**) Typical histograms of Sca-1/Flk-1 analysis for EPCs from normal (*db*/+) and type 2 diabetic (*db*/*db*) mice. (**B**) Type 2 diabetic *db*/*db* mice possess fewer circulating EPCs compared with normal *db*/+ mice (**P* < 0.05 vs. *db*/+, *n* = 4–5). (**C**) Type 2 diabetic mice exhibit elevated DHE fluorescent intensity in Sca-1/Flk-1–positive cells (**P* < 0.05 vs. *db*/+, *n* = 5).

Results

Circulating EPCs are reduced with increased intracellular superoxide in diabetic mice. Peripheral blood mononuclear cells were isolated from normal (*db*/+) and type 2 diabetic (*db*/*db*) mice, and the level of circulating EPCs was determined by Sca-1/Flk-1 staining. Flow analysis revealed a 59% decrease in circulating EPCs in diabetic mice (Figure 1, A and B). Previous studies have demonstrated that resistance of oxidative stress is important for normal EPC function (17, 18). To investigate whether circulating EPCs in type 2 diabetic mice exhibit elevated oxidative stress, blood mononuclear cells were isolated and stained with dihydroethidine/Sca-1/Flk-1 (DHE/Sca-1/Flk-1), followed by flow cytometry. The fluorescent intensity of DHE indicated the O_2^- level in Sca-1$^+$/Flk-1$^+$ cells. The results showed that O_2^- in circulating EPCs was increased by approximately 3 fold in diabetic mice (Figure 1C). These data suggest that type 2 diabetic mice have decreased circulating EPCs, characterized with elevated intracellular O_2^- levels.

Characterization of bone marrow–derived EPCs. To characterize bone marrow–derived EPCs, the stem cell markers (CD34, Sca-1), endothelial cell markers (Flk-1, VE-cadherin), and monocyte cell marker (CD11b) were examined using flow cytometry, based on the latest methods (22, 23). The cell population profiles of freshly isolated mononuclear cells (MNCs, day 0) and cultured cells (EPCs, day 7) are shown in Table 1. Compared with those of freshly isolated mononuclear cells, the percentages of CD34$^+$ cells and Sca-1$^+$ cells in cultured cells were increased approximately 2.5 fold and 3.4 fold, respectively. The Flk-1$^+$ cells and VE-cadherin$^+$ cells were increased approximately 5 fold and 2.3 fold, respectively. The Sca-1/Flk-1 double-positive cells were increased 2.7 fold (Table 1). There was no significant difference in the percentage of CD11b$^+$ cells between freshly isolated mononuclear cells and cultured cells. These data suggest that while the 7-day cultured EPCs are heterogeneous in nature, they contain significantly higher percentages of stem cells and endothelial cells compared with those of freshly isolated mononuclear cells. The 7-day cultured EPCs were also identified by 1,1′dioctadecyl-3,3,3′,3′-tetramethylindocarbocyanine perchlorate-labeled acetylated LDL/lectin (Dil-acLDL/lectin) double staining (Figure 2A). Additionally, the expressions of endothelial markers, comparing HUVECs and 7-day cultured EPCs, were determined using Western blot analysis. Similar to HUVECs, cultured EPCs expressed endothelial markers, including Flk-1, VE-cadherin, and eNOS (Figure 2, B and C), implying their potential in differentiating into endothelial lineage.

MnSOD expression is diminished in bone marrow–derived EPCs of diabetic mice and normal EPCs treated with high glucose. Major antioxidant enzymes, including MnSOD and catalase, are expressed in normal EPCs that protect their functions against oxidative stress (17, 18). Adult male *db*/*db* mice (10–14 weeks) exhibited hyperglycemia (389.24 ± 45.57 mg/dl; *n* = 25) compared with normal *db*/+ mice (168.36 ± 25.89 mg/dl; *n* = 25). To determine whether antioxidant enzymes were decreased in EPCs of type 2 diabetic mice, mRNAs of *MnSOD*, copper-zinc superoxide dismutase (*CuZnSOD*), and catalase (*Cat*) were examined using real-time PCR. The data showed that *MnSOD* mRNA was significantly decreased in EPCs of *db*/*db* mice (*db*/*db* EPCs), compared with that of normal EPCs from normal *db*/+ mice (*db*/+ EPCs) (Figure 3A). There were no significant differences in mRNA levels of *CuZnSOD* and *Cat*, between *db*/+ EPCs and *db*/*db* EPCs (Figure 3A). Consistent with real-time PCR results, both the protein level and enzymatic activity of MnSOD

Table 1
Characterizations of freshly isolated mononuclear cells and cultured EPCs

Markers	Day 0 (MNCs)	Day 7 (EPCs)
CD34	21.84 ± 3.02	50.96 ± 7.38[A]
Sca-1	17.42 ± 5.85	58.50 ± 10.20[A]
Flk-1	5.32 ± 0.30	24.06 ± 4.22[A]
Sca-1/Flk-1	4.98 ± 1.80	13.55 ± 1.27[A]
CD144	3.77 ± 0.46	8.76 ± 1.43
CD11b	65.40 ± 3.08	28.10 ± 1.13[A]

Characterizations of freshly isolated mononuclear cells (MNCs) and cultured EPCs. To characterize bone marrow–derived EPCs, the stem cell markers (CD34, Sca-1), endothelial cell markers (Flk-1, CD144), and monocyte marker (CD11b) were examined using flow cytometry. The day 0 (mononuclear cells) column shows characteristics of freshly isolated mononuclear cells, and the day 7 (cultured EPCs) column shows characteristics of 7-day cultured EPCs in EGM-2. *n* = 5 each group. [A]*P* < 0.05 vs. day 0 (mononuclear cells).

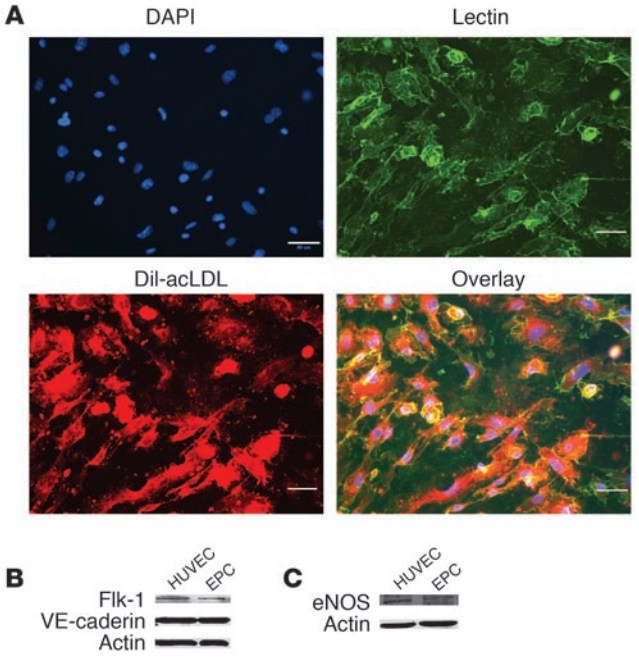

Figure 2
Characterization of mouse bone marrow–derived EPCs. (**A**) Staining of EPCs with acLDL (red) and lectin (green). The nuclei were counterstained with Hoechst (blue). Scale bar: 50 μm. (**B** and **C**) Expression of endothelial cell-specific markers in cultured EPCs. HUVECs were used as positive controls. (**B**) For Flk-1 and VE-cadherin, the loaded protein amount was 80 μg/lane. (**C**) For eNOS, the loaded protein amount was 30 μg/lane.

were significantly decreased in *db/db* EPCs compared with those of *db/+* EPCs (Figure 3, B–D). To examine the effect of high glucose on MnSOD expression, MnSOD protein was measured in normal EPCs treated with high glucose (25 mM, 400 mg/dl). The results showed that high-glucose treatment led to decreased MnSOD expression in normal EPCs (Figure 3, E and F). Taken together, these observations suggest that MnSOD is deficient in EPCs of type 2 diabetic mice, at least in part, due to hyperglycemia.

Mitochondrial oxidative stress is increased in EPCs from diabetic mice. Since MnSOD is an essential antioxidant enzyme in the mitochondrion (19), the level of mitochondrial oxidative stress (mtROS) in EPCs, indicated by MitoSOX fluorescence, was examined using flow cytometry (24). As shown in Figure 3, G and H, the levels of mtROS were significantly elevated in *db/db* EPCs (vs. *db/+* EPCs) as well as in normal EPCs treated with 25 mM high glucose (vs. *db/+* EPCs treated with 25 mM mannitol). To determine whether reduced MnSOD plays a role in increased mtROS, adenoviral vectors were used for gene transfer of MnSOD (Ad-MnSOD) or control GFP (Ad-GFP) into *db/db* EPCs. The results showed that MnSOD gene transfer blunted the elevation of mtROS in *db/db* EPCs (Figure 3H). Collectively, these data suggest that MnSOD deficiency is a critical factor for mtROS accumulation in diabetic EPCs.

Restoration of diabetic EPCs with ex vivo MnSOD gene therapy. To investigate EPC functions, EPC tube formation on Matrigel was examined to study its ex vivo angiogenic capacity. Bone marrow–derived EPCs were plated on Matrigel for 24 hours, and the number of tubes was counted. Diabetic EPCs formed significantly fewer networks than normal EPCs (Figure 4, A and B). Ex vivo gene therapy of *MnSOD* significantly improved the ability of *db/db* EPCs to form tube networks on Matrigel compared with unmodified *db/db* EPCs or the *db/db*-AdGFP EPC control (Figure 4, B–E). In contrast, when MnSOD expression was knocked down by its siRNA (downregulated by 60%–70% vs. normal EPCs, $P < 0.05$; $n = 3$), Matrigel tube formation was decreased by 52% compared with that of normal EPCs (Figure 4F). These data suggest that decreased MnSOD in *db/db* EPCs led to their diminished angiogenesis. In the process of repairing injured tissue, circulating EPCs adhere to connective tissue at the site of injury. EPCs isolated from *db/db* mice have previously been found to possess less ability to adhere to vitronectin. Consistent with a previous report (7), the adhesion of diabetic EPCs to vitronectin was significantly lower than that of normal EPCs (Figure 4G). Together, these findings demonstrate that gene therapy of *MnSOD* improved the angiogenic functions of diabetic EPCs.

Cell therapy of diabetic wounds with EPCs accelerates wound healing in diabetic mice. Diminished mobilization of EPCs from the bone marrow to the site of injury is one of the functional impairments of diabetic EPCs (8). Transplantation of EPCs to the local site could increase the number of EPCs at the site of injury and thus compensate for the diminished mobilization response in diabetic wound. The baselines of wound healing in both *db/db* mice and *db/+* mice were firstly determined. Each mouse underwent a single dorsal caudal 6-mm punch biopsy to create a full-thickness excisional wound. The rate of wound closure was then measured every other day until day 16. The data demonstrated that the wound closure in *db/db* mice was significantly delayed compared with that of *db/+* mice (Figure 5, A and D). To determine whether topical transplantation of EPCs onto the wounds of diabetic mice improves wound healing, either 1×10^6 normal EPCs (*db/+* EPCs) or 1×10^6 diabetic EPCs (*db/db* EPCs) were transplanted onto diabetic wounds immediately after wounding. Wound healing was significantly improved in the diabetic mice that received transplantation of either *db/+* EPCs or *db/db* EPCs (Figure 5, A and D). Wounds in *db/db* mice transplanted with *db/+* EPCs showed improved healing compared with untreated diabetic mice starting on day 4, whereas wounds in *db/db* mice receiving *db/db* EPC transplantation did not show a significant improvement until day 10 (both vs. *db/db* mice). The overall rate of wound healing was significantly greater in mice that received *db/+* EPCs when compared with mice that received *db/db* EPC transplantation. These data suggest that, while transplantation of EPCs from diabetic mice improved the rate of wound healing, diabetic EPCs were less effective in accelerating wound healing than normal EPCs.

MnSOD gene therapy of diabetic EPCs augments in vivo function of transplanted EPCs in diabetic wound healing. The data described above showed that EPCs isolated from *db/db* mice had decreased MnSOD and elevated mtROS levels. *MnSOD* gene therapy of diabetic EPCs improved their ex vivo tube formation and ameliorated elevated mtROS. To determine whether MnSOD could improve in vivo angiogenic function of diabetic EPCs and accelerate wound healing, *MnSOD* gene therapy of diabetic EPCs (*db/db*-AdMnSOD EPCs) was performed prior to transplantation, and GFP gene transfer to diabetic EPCs (*db/db*-AdGFP EPCs) served as controls. EPCs from *db/db* mice transfected with Ad-MnSOD augmented wound healing, starting on day 6 (vs. *db/db* mice only and *db/db* mice treated with *db/db*-AdGFP EPCs) (Figure 5, B and D). The

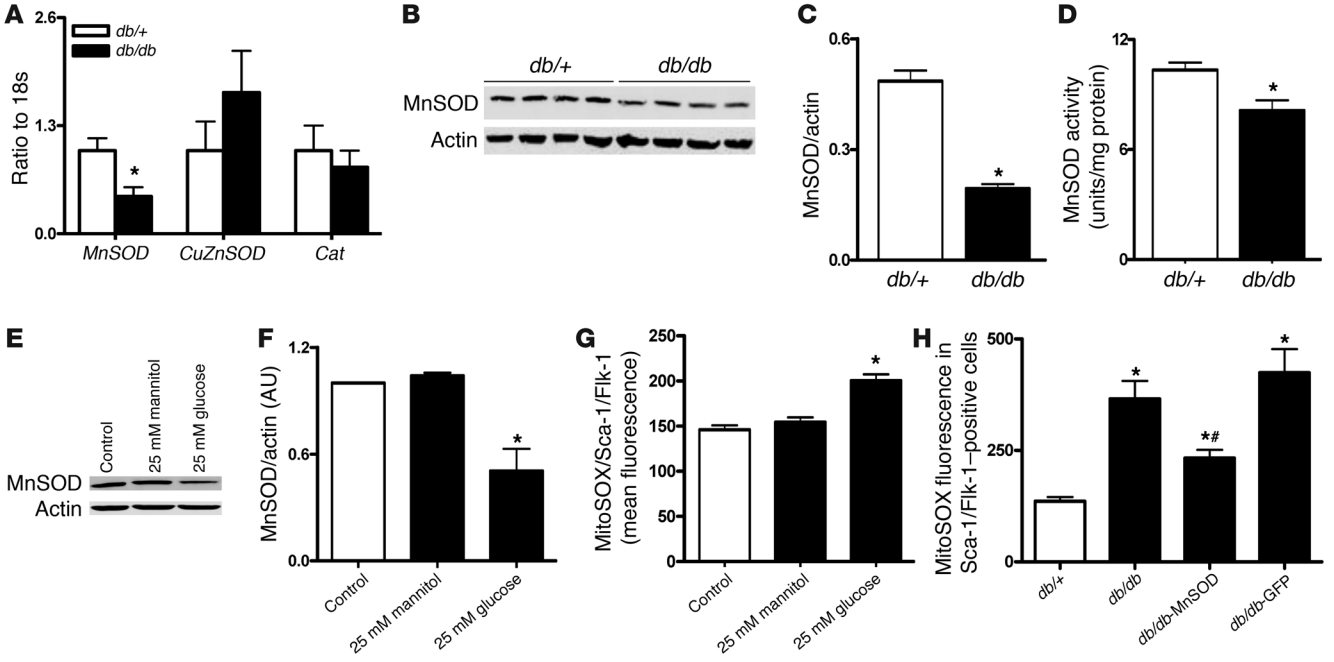

Figure 3

Expression of antioxidant enzymes in bone marrow EPCs. (**A**) mRNA levels for *MnSOD*, *CuZnSOD*, and *Cat*, quantified by real-time PCR. Only the *MnSOD* mRNA level was significantly decreased in EPCs of type 2 diabetic (*db*/*db*) mice (**P* < 0.05 vs. *db*/+ EPCs, *n* = 5). (**B** and **C**) Western blot analysis demonstrating, diminished the MnSOD protein levels in *db*/*db* EPCs (**P* < 0.05 vs. *db*/+ EPCs, *n* = 4). (**D**) Reduced MnSOD enzymatic activity in *db*/*db* EPCs (**P* < 0.05 vs. *db*/+ EPCs, *n* = 4–7). (**E**–**G**) High-glucose treatment reduced MnSOD expression and increased mtROS in normal EPCs (*db*/+ EPCs [control]) (**P* < 0.05 vs. control or 25 nM mannitol-treated group, *n* = 5). (**H**) mtROS was elevated in EPCs of type 2 diabetic (*db*/*db*) mice (**P* < 0.05 vs. *db*/+ EPCs, *n* = 5). Gene transfer of MnSOD (*db*/*db*-MnSOD), but not GFP (*db*/*db*-GFP), blunted the mtROS level in EPCs of *db*/*db* mice (#*P* < 0.05 vs. *db*/*db* EPCs, *n* = 5).

overall rate of wound healing was significantly accelerated in *db/db* mice that received *db/db*-AdMnSOD EPCs when compared with that of *db/db* mice without cell transplantation or *db/db* mice that received *db/db*-AdGFP EPC transplantation (Figure 5, B and D). These data suggest that diabetic EPCs after *MnSOD* gene therapy are more effective in accelerating wound repair than the same number of diabetic EPCs without *MnSOD* gene therapy. To further investigate the role of MnSOD on angiogenesis in vivo, MnSOD was knocked down by its siRNA in normal EPCs (*db/*+-siMnSOD EPCs). MnSOD expression in normal EPCs was decreased by 60%–70% after treatment with MnSOD siRNA, which was confirmed using Western blot analysis ($P < 0.05$; $n = 3$). Transplantation of *db/*+-MnSOD-siRNA EPCs failed to improve wound healing in *db/db* mice compared with that of *db/*+ EPCs or *db/db*-AdMnSOD EPCs (Figure 6, A and B). Mice receiving *db/*+-MnSOD-siRNA EPC therapy showed similar pace compared with diabetic EPC-induced wound closure (Figure 6, A and B). Together, these data suggest that MnSOD is a key component for normal EPC-induced angiogenesis in diabetic wound healing.

Increasing the number of transplanted diabetic EPCs, together with ex vivo MnSOD gene therapy, further accelerates diabetic wound healing. Compared with 1×10^6 normal EPCs, the same number of diabetic EPCs transfected with Ad-MnSOD was less effective in accelerating diabetic wound closure. To investigate whether twice the number of transplanted EPCs would compensate for the existing EPC dysfunction and further accelerate wound healing, 2×10^6 EPCs (either *db/db*-AdGFP EPCs or *db/db*-AdMnSOD EPCs) were topically transplanted on 6-mm punch wounds in *db/db* mice. The results showed that transplantation of 2×10^6 *db/db*-AdGFP EPCs significantly improved the rate of wound healing compared with that of 1×10^6 *db/db*-AdGFP EPCs or 1×10^6 diabetic EPCs. Interestingly, for improving wound healing in *db/db* mice, transplantation of 1×10^6 *db/db*-AdMnSOD EPCs had an equivalent effect to that of 2×10^6 *db/db*-AdGFP EPCs. Importantly, transplantation of 2×10^6 *db/db*-AdMnSOD EPCs resulted in significantly accelerated wound healing compared with that of 2×10^6 *db/db*-AdGFP EPCs in *db/db* mice (Figure 5, C and D). Comparing multiple groups, we found that transplantation of 2×10^6 *db/db*-AdMnSOD EPCs significantly improved the closure of diabetic wounds compared with that of 1×10^6 *db/db*-AdMnSOD EPCs, 2×10^6 *db/db*-AdGFP EPCs, and 2×10^6 *db/db* EPCs as well as the untreated *db/db* control mice. The rate of wound closure compared among groups with transplantation of 2×10^6 *db/db*-AdMnSOD EPCs and 1×10^6 *db/*+ EPCs or the control *db/*+ mice was equivalent. Collectively, these data provide the evidence that although angiogenic function in diabetic EPCs is impaired, supplementation of exogenous MnSOD and increasing EPC number together can fully rescue MnSOD-mediated EPC dysfunction in diabetic angiogenesis and wound healing.

EPC therapy of diabetic wounds augments in vivo angiogenesis with early accelerated wound healing. Wounds and surrounding skin tissues were recovered, and the capillaries were stained for CD31. On day 3 of wound healing, capillary formation was significantly greater in normal mice compared with all other groups (Figure 7A). On day 6 of wound healing, normal mice continued to show significantly more capillary formation compared with *db/db* mice with-

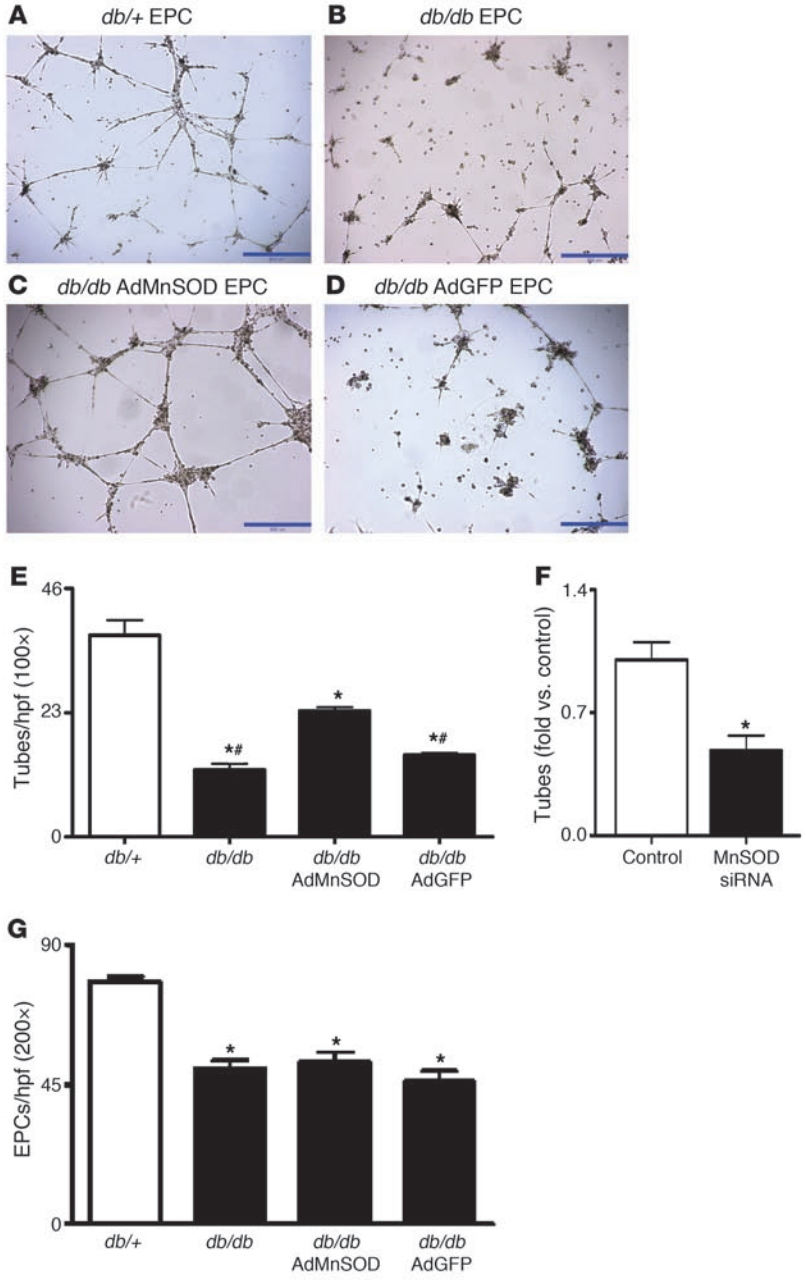

Figure 4
EPC functional assays. Typical photographs of tube formation on Matrigel for (**A**) normal EPCs (*db*/+ EPCs), (**B**) type 2 diabetic EPCs (*db*/*db* EPCs), (**C**) type 2 diabetic *db*/*db* EPCs upon *MnSOD* gene therapy, and (**D**) type 2 diabetic *db*/*db* EPCs transfected with GFP control. (**B**–**D**) Representative photographs were of EPCs isolated from the same *db*/*db* mouse. Scale bar: 650 μm. (**E**) *MnSOD* gene therapy, but not that of the GFP control, improved the ability of *db*/*db* EPCs to form tubes on Matrigel (**P* < 0.05 vs. *db*/+ EPCs, #*P* < 0.05 vs. *db*/*db*-MnSOD, *n* = 5). Scale bar: 650 μm. (**F**) MnSOD knockdown by MnSOD siRNA significantly inhibited EPC-induced Matrigel tube formation (**P* < 0.05 vs. control, *n* = 3). (**G**) Adhesion to vitronectin was impaired in *db*/*db* EPCs. *MnSOD* gene therapy of *db*/*db* EPCs had no effect on EPC adhesion (**P* < 0.05 vs. *db*/+ EPCs, *n* = 5). hpf, high-power field.

out EPC therapy or *db/db* mice with *db/db* EPC or *db/db*-AdGFP EPC therapy (Figure 7B and Figure 8). However, *db/db* mice treated with 1 × 10^6 *db/+* EPCs, 1 × 10^6 *db/db*-AdMnSOD EPCs, 2 × 10^6 *db/db*-AdMnSOD EPCs, or 2 × 10^6 *db/db*-AdGFP EPCs demonstrated significantly more capillary formation compared with nontreated *db/db* controls on day 6 (Figure 7B). On day 16 of wound healing, diabetic mice continued to show significantly less capillary formation than all other groups (Figure 7C). Conversely, treatment groups that demonstrated accelerated wound healing compared with nontreated *db/db* mice showed significantly more capillary formation on day 6 (Figure 7B and Figure 8). Genetically modifying diabetic EPCs with MnSOD (*db/db*-AdMnSOD EPCs) and/or increasing the number of *db/db* EPCs from 1 × 10^6 to 2 × 10^6 (*db/db*-AdGFP EPCs) improved the ability of transplanted diabetic EPCs to enhance capillary formation. These data demonstrate that restoration of EPC function with MnSOD prior to transplant or increasing the number of transplanted diabetic EPCs is an effective means to enhance angiogenesis in diabetic wound healing. The structures of skin capillaries were further confirmed by CD34 (Figure 8, Q and R) and vWF staining (Figure 8, S and T).

Transplanted EPCs integrate into cutaneous vasculature and surrounding tissue. To determine where transplanted EPCs were integrating, EPCs isolated from *db/+* mice were incubated with BrdU, starting on day 5 of cell culture. After 7 days of culture, 2 × 10^6 EPCs were transplanted onto a 6-mm punch biopsy wound of a *db/db* mouse at the time of wounding. On day 6 of wound healing, the wound and surrounding skin tissues were recovered and stained for BrdU-positive cells. The data showed that BrdU-labeled EPCs integrated into vascular-like structures and the dermis (Figure 9, A–D). To verify that BrdU-labeled EPCs were incorporated into the capillary wall, the wound tissue slides were stained with EC-specific marker CD31, followed by BrdU staining. As shown in Figure 9, E–H, some BrdU-positive cells (red fluorescence) were integrated into CD31-positive vessels (green fluorescence). The remaining BrdU-positive cells were found surrounding the vessels. Previous studies have shown that bone marrow–derived progenitor cells integrate into multiple structures in skin (25, 26). Our present findings suggest that topically delivered EPCs participate in wound angiogenesis, by either directly forming capillary with existing endothelial cells or acting in a paracrine fashion to induce angiogenesis via surrounding endothelium.

EPC-conditioned culture media on diabetic wound healing. To study the paracrine effect of EPCs on wound healing, the conditioned culture media of normal (*db/+* EPCs) and diabetic EPCs (*db/db* EPCs) were collected and applied to diabetic wounds. The results showed that both normal and diabetic culture media accelerated diabetic wound healing from day 10 to day 16 without significant difference, compared with control media alone (Figure 10, A and B).

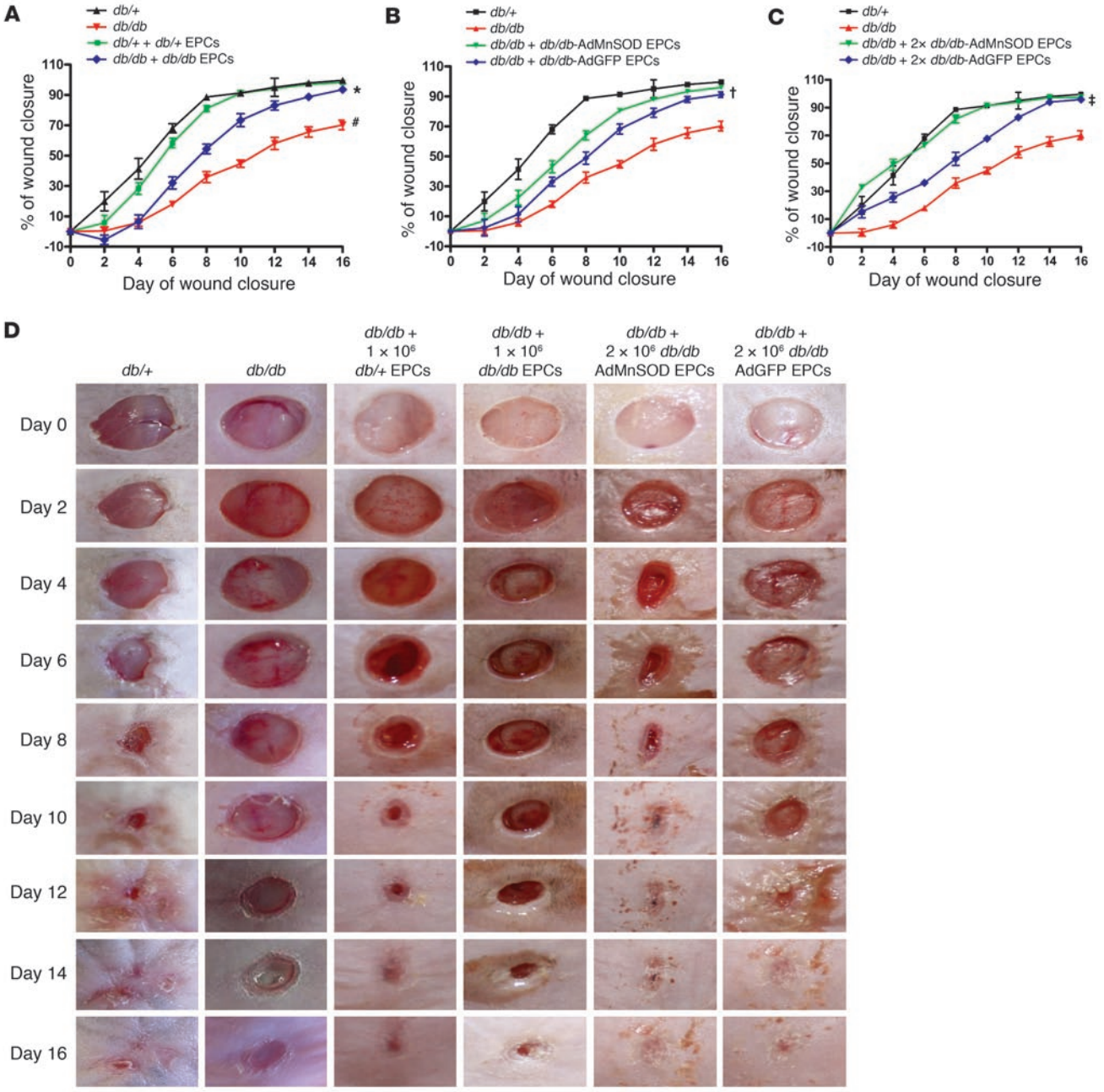

Figure 5

EPC therapy of diabetic wounds improved the rate of wound closure in type 2 diabetic mice. The closure rate of 6-mm punch biopsies was measured every other day until day 16. Wound healing of normal *db*/+ mice and type 2 diabetic *db*/*db* mice represent the baseline, are the same for **A**–**C**, and represent the control groups. (**A**) For *db*/+ and *db*/*db* mice that were transplanted with 1×10^6 *db*/+ EPCs, EPCs significantly improved the rate of wound closure in *db*/+ mice compared with that of *db*/*db* mice transplanted with 1×10^6 *db*/*db* EPCs ($^*P$ 0.01 and $^{\#}P < 0.01$ vs. 1×10^6 *db*/*db* EPCs, $n = 10$ each group). Wounds of *db*/+ and *db*/*db* mice transplanted with 1×10^6 *db*/+ EPCs healed at equivalent rates ($P = 0.185$ vs. 1×10^6 *db*/+ EPCs, $n = 10$ each group). (**B**) *MnSOD* gene therapy of EPCs prior to transplantation (1×10^6 *db*/*db*-AdMnSOD EPCs) significantly improved *db*/*db* EPC ability to ameliorate wound closure versus transplantation of 1×10^6 control GFP *db*/*db* EPCs (*db*/*db*-AdGFP EPCs) ($^{\dagger}P < 0.01$ vs. 1×10^6 *db*/*db*-AdGFP EPCs, $n = 10$ each group). (**C**) Transplantation of 2×10^6 *db*/*db*-AdMnSOD EPCs significantly improved the rate of wound closure versus that of 2×10^6 *db*/*db*-AdGFP EPCs ($^{\ddagger}P < 0.05$ vs. 2×10^6 *db*/*db*-AdGFP EPCs, $n = 10$ each group). No difference was found in the rate of wound closure among 2×10^6 *db*/*db*-AdMnSOD EPCs and 1×10^6 *db*/+ EPCs or in *db*/+ mice. Transplantation of 2×10^6 *db*/*db*-AdMnSOD EPCs significantly improved the rate of wound closure in *db*/*db* mice versus that of other cell therapy groups (i.e., 1×10^6 *db*/*db* EPCs, 1×10^6 *db*/*db*-AdMnSOD EPCs, and 1×10^6 *db*/*db*-AdGFP EPCs). (**D**) Typical photographs of wound healing for above groups.

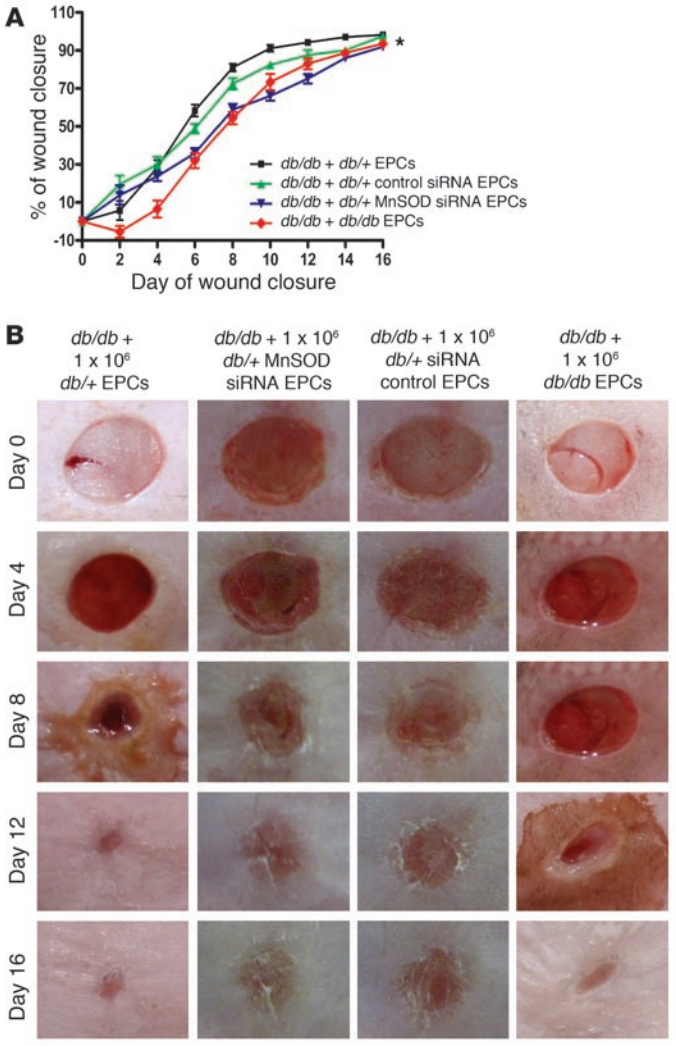

Figure 6
MnSOD deficiency impedes EPC-mediated wound healing in normal mice. (**A**) MnSOD knockdown by its siRNA in normal EPCs (1×10^6 *db*/+-MnSOD-siRNA EPCs) significantly decreased their ability to ameliorate wound closure versus that of 1×10^6 *db*/+-control-siRNA EPCs (*$P < 0.01$ vs. 1×10^6 *db*/+-control-siRNA EPCs, $n = 6$). (**B**) Typical photographs of wound healing.

However, the overall rates of wound healing in *db/db* mice receiving the conditioned media could not reach the healing rate of the normal EPC-transplanted group in *db/db* mice. These data suggest that both normal and diabetic EPCs exert paracrine effects on diabetic wound healing, in additional to their direct angiogenic effects.

Discussion

The major findings in this study are that (a) the expression and activity of MnSOD are diminished in diabetic EPCs, paralleled with increased mitochondrial superoxide and decreased angiogenic functions; (b) topical delivery of diabetic EPCs has less efficiency than that of normal EPCs in accelerating wound healing in diabetic mice; (c) ex vivo gene therapy of diabetic EPCs impedes increased mitochondrial superoxide and rescues impaired angiogenic functions in vitro and in vivo, resulting in accelerated wound healing in type 2 diabetic mice.

Wound healing is an integrative and well-coordinated regenerative response to tissue injury that involves a complex interaction and cross-talk of various cell types, extracellular matrix molecules, soluble mediators, and cytokines (2). Despite the evidence shown by recent studies that local or systematic administration of cells and/or proangiogenic molecules could significantly improve angiogenesis and wound closure, refractory diabetic wounds remain a significant clinical problem, leading to limb amputation (2). EPCs, as important precursors of endothelial cells, have been demonstrated to be involved in angiogenesis and wound repair. Treatments with sonic hedgehog or stromal cell–derived factor-1α accelerate wound healing in diabetes by enhancing NO (27) and EPC-mediated angiogenesis (7, 8). These studies have shed new light on autologous EPC therapy for diabetic wounds and ischemia heart disease. However, recent clinical trials of EPC therapy for ischemic/injured tissues have revealed that autologous progenitor cell therapy for diabetic patients is not as effective in repairing ischemic/injured tissue as autologous cell therapy for nondiabetic patients (11, 28). The outcomes from these clinical studies indicate that EPC function and recruitment are fundamentally impaired in diabetic and other ischemic diseases, which impedes the efficiency of EPC-based cell therapy (9, 11). Hence, EPCs from patients with chronic diseases are dysfunctional and contribute to inefficient therapeutic outcomes in the clinic setting. This stipulation is verified by the present study, showing that (a) the number of circulating EPCs was significantly reduced in diabetic mice, suggesting inadequate EPC mobilization from their bone marrow; (b) EPCs isolated from diabetic mice had reduced Matrigel tube formation and adhesion ability, indicating attenuated ex vivo angiogenesis; (c) topical application of diabetic EPCs onto the diabetic wounds exhibited less efficiency on capillary formation and wound repair than that of the same number of normal EPCs, implicating diminished in vivo vasculogenesis. This evidence suggests that diabetic EPCs are defective in mobilization and angiogenesis, contributing to impaired wound healing in diabetes. In the present study, we focused on the mechanisms of EPC dysfunction and its role on wound repair in type 2 diabetic mice, which may provide another consideration for the use of progenitor cells therapeutically.

It is well known that ROS production is an important mediator of hyperglycemia-mediated endothelial cell damage. We have previously demonstrated that cutaneous MnSOD protein and enzymatic activity were significantly decreased in both STZ-induced type 1 diabetic mice and $Ins2^{Akita}$ type 1 diabetic mice. Topical gene therapy of *MnSOD* onto the diabetic wounds significantly increased cutaneous MnSOD activity throughout the wound healing process in STZ mice, accelerating wound closure (15). Normal EPCs possess high intrinsic levels of antioxidant enzymes such as MnSOD, which confer protection against oxidative stress (18). The present study demonstrated that there was increased mtROS accumulation with diminished in vitro angiogenesis in diabetic EPCs, implicating that excessive mtROS may damage EPC angiogenesis functions. The expression and enzymatic activity of MnSOD were significantly decreased in diabetic EPCs, suggesting that such deficiencies render diabetic EPCs ineffective in scavenging elevated mtROS. Although we found that intracellular antioxidant enzymes, including catalase and CuZnSOD, were not decreased in

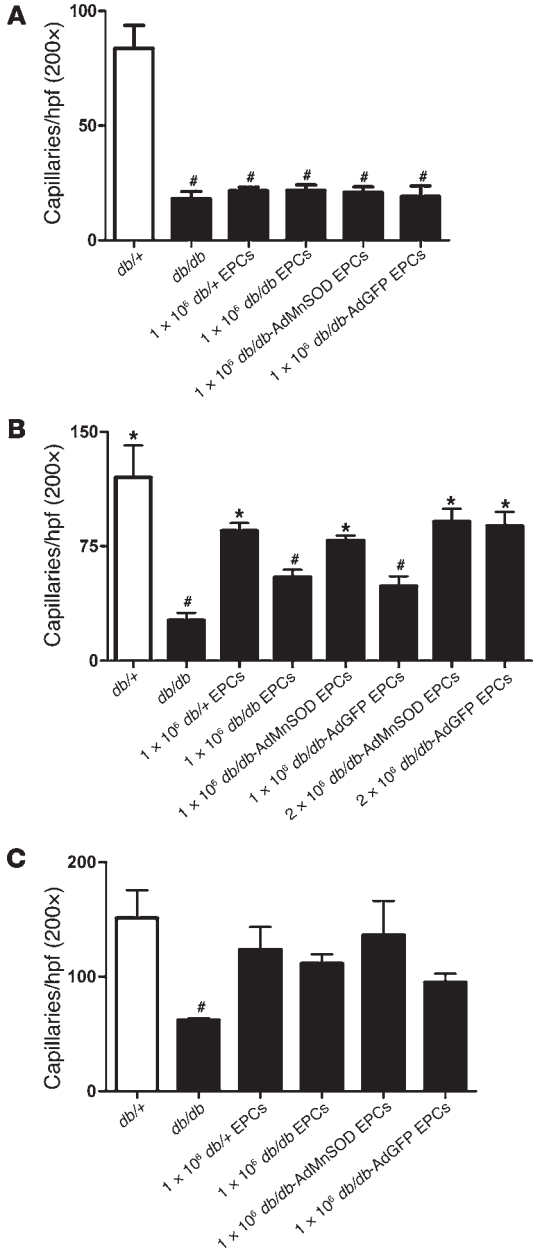

Figure 7
Wound angiogenesis after 6-mm punch biopsy. (**A**) There were significantly more wound capillaries in *db*/+ mice compared with those of all *db*/*db* groups on day 3 ($^{\#}P < 0.05$). (**B**) On day 6 of wound healing, wound angiogenesis was increased in *db*/+ and *db*/*db* mice treated with 1×10^6 EPCs isolated from *db*/+ mice (*db*/+ EPCs) and *db*/*db* mice after *MnSOD* gene therapy (1×10^6 *db*/*db*-AdMnSOD EPCs) or treatment with 2×10^6 EPCs from *db*/*db* mice after *MnSOD* gene therapy (2×10^6 *db*/*db*-AdMnSOD EPCs) or GFP control (2×10^6 *db*/*db*-AdGFP EPCs) compared with that of *db*/*db* mice ($^{*}P < 0.05$ vs. *db*/*db* mice). *db*/*db* mice without cell therapy and *db*/*db* mice treated with 1×10^6 EPCs from *db*/*db* mice (*db*/*db* EPCs) and GFP control (1×10^6 *db*/*db*-AdGFP EPCs) demonstrated significant less wound angiogenesis compared with that of *db*/+ mice ($^{\#}P < 0.05$ vs. *db*/+ mice). (**C**) *db*/*db* mice demonstrated significantly less wound angiogenesis compared with that of normal *db*/+ mice ($^{\#}P < 0.05$ vs. *db*/+ mice) on day 16. $n = 4–5$ in each group.

diabetic EPCs, they apparently failed to compensate for the damage by excessive ROS and protected EPCs against angiogenic dysfunctions in this model. Recent studies have shown that *MnSOD* gene transfer could significantly reduce irradiation esophagitis by enhancing the self-renewal of bone marrow–derived progenitor cells (29), raising the possibility that local delivery of gene-modified EPCs onto the diabetic wounds may accelerate wound healing. In agreement with this notion, our results showed that restoration of MnSOD retarded mtROS accumulation and rescued the impaired ex vivo tube formation of diabetic EPCs. Furthermore, gene therapy of *MnSOD* significantly improved diabetic EPC-mediated angiogenesis, with subsequent acceleration of diabetic wound closure. Conversely, downregulation of MnSOD by its siRNA in normal EPCs decreased Matrigel tube formation in vitro and impeded their ability on diabetic wound repair in vivo, when compared with normal EPC controls. These observations strongly suggest that MnSOD deficiency is an important mechanism underlying the susceptibility of diabetic EPCs to high glucose-induced superoxide, resulting in diabetic EPC dysfunctions.

Another interesting finding in our study is that when the number of transplanted, MnSOD-modified diabetic EPCs (*db/db*-AdMnSOD EPCs) was increased from 1×10^6 to 2×10^6, wound closure rate and capillary density reached the same levels as those of 1×10^6 normal EPCs. Furthermore, 2×10^6 *db/db*-AdGFP EPCs significantly improved wound healing and angiogenesis compared with *db/db* mice with or without *db/db* EPC therapy. In the present study, we chose 1×10^6 cells as the initial dose for topical cell therapy on a 6-mm biopsy wound, based on previous studies demonstrating that transplantation of 1×10^5 EPCs to normal mice significantly accelerated dermal wound healing compared with mature endothelial cells (26). Considering the established evidence that wound healing is delayed in diabetic patients and animal models, we increased our initial cell therapy regimen to 1×10^6 EPCs in order to ascertain their effects on diabetic wound repair. Although only 2 cell therapy regimens were compared, our studies suggest that topical delivery of MnSOD gene-modified EPCs or an increased number of autologously transplanted EPCs is an efficacious means to accelerate wound healing in diabetes. Future studies are warranted to determine the optimal cell regimens by considering cell density and the size of the wound area.

Angiogenesis is a vital component of wound repair. EPCs are involved in multiple aspects of angiogenesis to affect the wound healing process. EPCs can differentiate into endothelial lineage and incorporate into the existing vascular structure to participate in neovascularization (30, 31). They can also secret cytokines and growth factors, including VEGF, FGF, and IGF-1, in a paracrine fashion to induce sprouting angiogenesis by the surrounding endothelium (30–32). Indeed, our immunohistochemical assay indicated that while some EPCs were integrated into the vascular wall, the remaining EPCs were found surrounding the vessels. Local treatment with EPC-conditioned media also resulted in improved wound healing in diabetic mice. Combining the morphological and in vivo angiogenesis evidence, our findings suggest that topically delivered EPCs participate in angiogenesis and wound healing by either direct incorporation into the preexisting vascular structures or acting in a paracrine pattern to improve neovascularization by the surrounding endothelium. Of note,

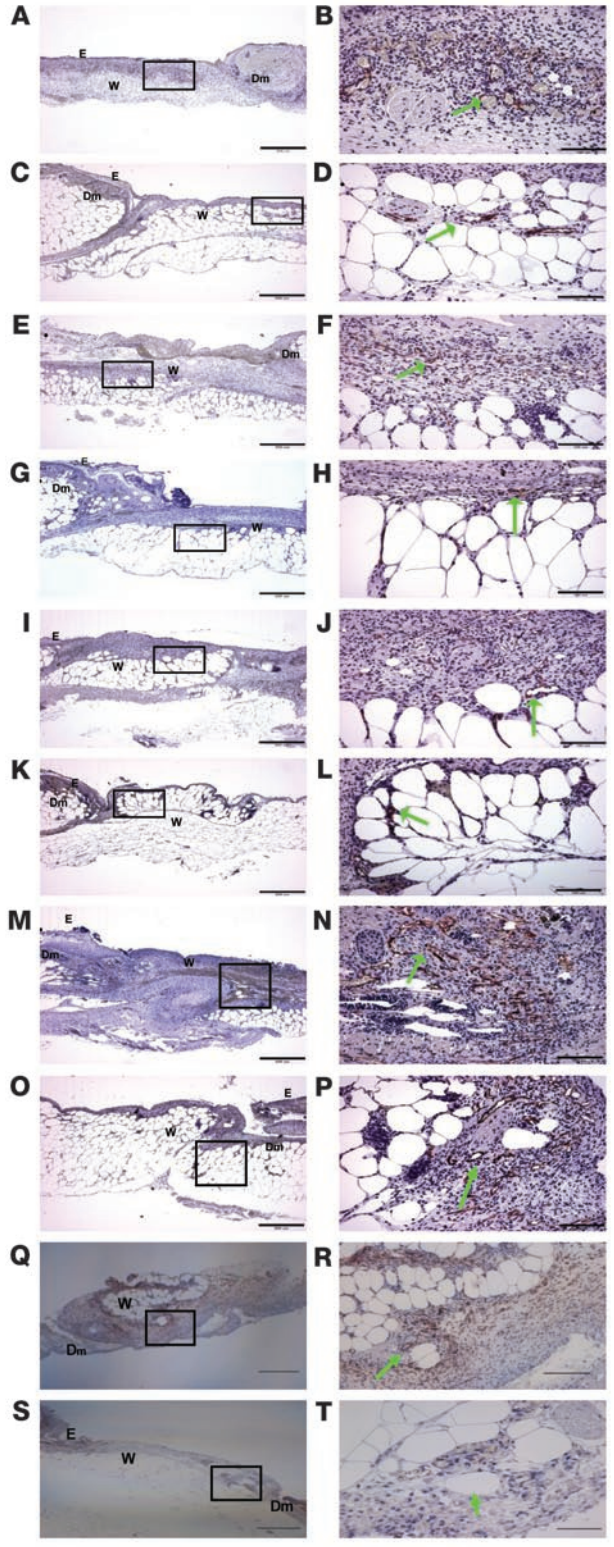

Figure 8
Typical photographs of CD31 staining on day 6 of wound healing. (**A** and **B**) *db*/+ mice, (**C** and **D**) *db*/*db* mice, and (**E** and **F**) *db*/*db* mice, with EPC therapy of 1×10^6 *db*/+ EPCs, (**G** and **H**) *db*/*db* EPCs, (**I** and **J**) *db*/*db*-AdMnSOD EPCs, (**K** and **L**) *db*/*db*-AdGFP EPCs, (**M** and **N**) 2×10^6 *db*/*db*-AdMnSOD EPCs, and (**O** and **P**) 2×10^6 *db*/*db*-AdGFP EPCs. Green arrows point to CD31-positive capillaries. (**Q** and **R**) Typical photographs of CD34 staining on day 6 of wound healing in *db*/+ mice. Green arrows point to CD34-positive capillaries. (**S** and **T**) Typical photographs of vWF staining on day 6 of wound healing in *db*/+ mice. Green arrows point to vWF-positive capillaries. Boxed regions are shown at higher magnification to the right. Statistic analyses are shown in Figure 7B. W, wound; Dm, dermis; E, epidermis. Scale bar: 500 μm (**A**, **C**, **E**, **G**, **I**, **K**, **M**, **O**, **Q**, and **S**); 100 μm (**B**, **D**, **F**, **H**, **J**, **L**, **N**, **P**, **R**, and **T**). Original magnification, ×40 (**A**, **C**, **E**, **G**, **I**, **K**, **M**, **O**, **Q**, and **S**); ×200 (**B**, **D**, **F**, **H**, **J**, **L**, **N**, **P**, **R**, and **T**).

there is no difference in wound closure between diabetic EPC-conditioned media and normal EPC-conditioned media, which may be due to the complex interaction between the host tissue microenvironments and growth factors secreted by transplanted EPCs. However, diabetic EPCs induced less capillary formation in diabetic wounds compared with that of normal EPCs. Gene therapy of *MnSOD* or doubling the transplanted EPC number also significantly enhanced capillary formation. Although it is unclear whether the improvement upon EPC therapy is exclusively mediated by EPC integration or paracrine effects, these results imply that the significant differences between normal and diabetic EPC therapies are mainly due to EPC dysfunction, since *MnSOD* gene therapy rescued EPC dysfunction and improved their angiogenesis function on wound healing.

In the present study, *db/db* mice, which possess an inactivating mutation of the gene encoding leptin receptors and subsequently develop obesity, insulin resistance, and diabetes with hyperglycemia resembling adult-onset diabetes mellitus (33), were used as a type 2 diabetic model. Although leptin has been shown to promote vascular remodeling in *db/db* mice (34) and different concentrations of leptin affect EPC function in vitro (35), *db/db* mice are a well-established model for studying the effect of hyperglycemia on EPC function and wound healing (36, 37). In the present study, EPCs isolated from diabetic mice exhibited impaired functions, including decreased MnSOD, tube formation, adhesion, and regenerative capacity in wound closure. Our ex vivo results provided further supporting evidence that normal EPCs treated with high glucose had decreased MnSOD and increased mtROS in culture. These observations support the concept that hyperglycemia is a key factor for EPC dysfunction in diabetes. Our study also demonstrated that EPCs isolated from animal models of diabetes maintained persistent dysfunction despite being cultured in euglycemic cell media, a process we termed "cytomneosis" (Greek for cell memory of disease). Our findings are consistent with previous studies showing such dysfunction persists in daughter cells of diabetic EPCs after 7 days of cell culture in euglycemic media in which cell proliferation took place (38, 39). The mechanism for cytomneosis and/or heritable dysfunction from parent to daughter cells is currently under study and remains to be fully elucidated.

In summary, the present study demonstrates that EPCs of type 2 diabetic mice possess impaired angiogenesis functions, paralleled by increased mtROS and diminished expression and activity of MnSOD, which can be partially rescued via *MnSOD* gene therapy. Restoration of diabetic EPC functions with *MnSOD* gene therapy prior to their transplantation or increasing the number of transplanted diabetic EPCs results in enhanced wound angiogenesis and accelerated wound closure. For the development of novel cell therapies for diabetic patients, improvement in progenitor cell

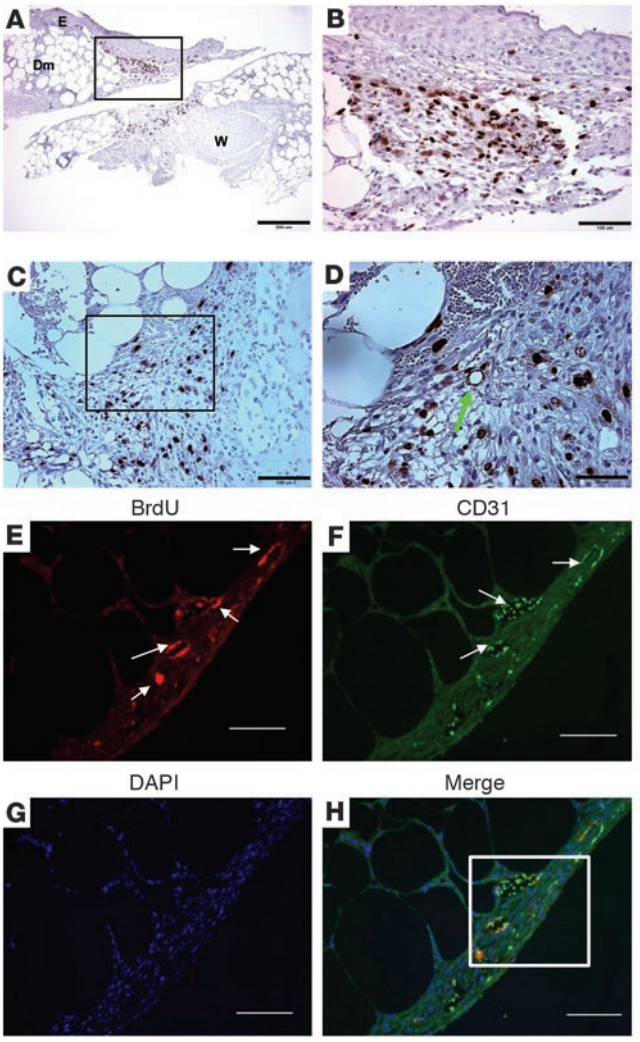

Figure 9
In vivo integration of transplanted EPCs on day 6 of wound healing. At the time of wounding, 2×10^6 BrdU-labeled *db*/+ EPCs were transplanted onto 6-mm punch biopsy wounds of *db*/*db* mice. On day 6 of wound healing, wounds were isolated, fixed, and stained for BrdU (brown stained cells). (**A**–**D**) Typical photographs demonstrate EPC integration into the dermis and vascular structure. Boxed regions are shown at higher magnification to the right. The green arrow points to BrdU-positive capillaries. Scale bar: 500 μm (**A**); 100 μm (**B** and **C**); 50 μm (**D**). (**E**–**H**) To ascertain that BrdU-labeled EPCs were incorporated into the capillary wall, wound tissues were stained for CD31, followed by BrdU staining. Typical photographs indicate that some BrdU-positive cells (red fluorescence) (**E**) were incorporated into CD31-positive vessels (green fluorescence) (**F**). White arrows point to CD31-positive cells. Remaining BrdU-positive cells surrounded the vessels. (**G**) The nucleus was counterstained with DAPI (blue fluorescence). The merged image is shown in **H**. The white boxed region indicates CD31/BrdU double-positive cells. Scale bar: 100 μm. Original magnification, ×40 (**A**); ×200 (**E**–**H**); ×200 (**B** and **C**); ×400 (**D**).

function through gene therapy prior to transplantation and/or increasing the number of transplanted cells may be necessary to compensate for their dysfunction.

Methods

Mouse model of diabetes. The *db*/*db* mouse is an established model to study angiogenesis and vascular dysfunction in type 2 diabetes (33–36). Mice used in this study were adult male diabetic (*db*/*db*, BKS.Cg-m$^{-/-}$ *Lepr*^{db}/Bom Tac) and nondiabetic healthy heterozygotes (*db*/+, BKS.Cg-m$^{-/-}$ *Lepr*^{db}/– lean) (9) purchased from The Jackson Laboratory (10–14 weeks old). Criteria for inclusion were a blood glucose level of less than 200 mg/dl (normal, *db*/+) and a blood glucose level of more thsan 300 mg/dl (type 2 diabetic, *db*/*db*). All animal procedures were performed with approval of the University of Pittsburgh Institutional Animal Care and Use Committee.

Isolation and characterization of mouse EPCs from blood and bone marrow. EPCs were isolated from blood and bone marrow of both normal *db*/+ and type 2 diabetic *db*/*db* mice, according to established methods with minor modifications (22, 23). Mice were anesthetized with gas anesthesia (O_2, 1 l/min; N_2O, 0.4 l/min; isoflurane, 0.5–1 l/min). Peripheral blood (0.5–1 ml) was collected from a cardiac puncture into a 1-ml syringe containing 100:l heparin (1,000 units/ml; Sigma-Aldrich). Mononuclear cells were isolated from blood with Histopaque 1083 (Sigma-Aldrich) density gradient centrifugation (800 *g*, 4°C) for 30 minutes. The mononuclear fraction was removed, centrifuged (400 *g*, 4°C), and red blood cells were lysed with ammonium chloride solution (Stemcell Technologies), washed 3 times (400 *g*, 4°C) in PBS with 1% albumin, and then used for testing by flow cytometry.

Bone marrow was flushed out of the tibias and femurs with EGM-2 using a 25-gauge needle, separated with vigorous pipetting, and then centrifuged for 5 minutes (400 *g*, 4°C). Red blood cells were lysed with ammonium chloride solution (Stem Cell Technologies) and washed 3 times in EGM-2 (400 *g*, 4°C). Cells were plated in a vitronectin-coated (Sigma-Aldrich) 6-well plate at 8.5×10^5 cell/cm^2 in EGM-2 (VEGF, hydrocortisone, hFGF, IGF, ascorbic acid, hEGF, heparin, and 5% FBS) (Lonza) at 37°C, 5% CO_2. After 4 days in culture, nonadherent cells were removed, and new EGM-2 was changed daily. All cells used in molecular assays were performed after day 7.

Freshly isolated mononuclear cell and cultured bone marrow–derived EPCs were characterized using flow cytometry, based on established methods (22, 23). Briefly, 1×10^6 cells were resuspended in 100 μl 1% BSA/PBS, incubated with PE-conjugated CD34, FITC-conjugated CD144, PE-conjugated CD11b, FITC-conjugated Sca-1, and PE-conjugated Flk-1 in the dark for 1 hour on ice. Quantifications of Sca-1$^+$/Flk-1$^+$, CD34$^+$, CD144$^+$, and CD11b$^+$ cells were performed with a BD Vantage Flow Cytometer. To confirm the EPC phenotypes, after 7-day culture attached cells were labeled with Dil-acLDL (10 μg/ml; Invitrogen) and FITC-labeled *Ulex europaeus* agglutinin (lectin, 10 μg/ml; Sigma-Aldrich) for 1 hour. After nuclei staining by Hoestch (5 μg/ml; Sigma-Aldrich), cells were viewed under an inverted fluorescent microscope (Nikon). Pictures were taken under high-power fields (magnification, ×200). Cells demonstrating double-positive fluorescence of Dil-acLDL and lectin were identified as differentiating EPCs. In addition, the expression of Sca-1, Flk-1, CD34, VE-cadherin (CD144), and CD11b were analyzed using flow cytometry and compared with freshly isolated mononuclear cells (Table 1). EPCs were gently detached using 5 mmol/l EDTA/PBS at 37°C, washed, and incubated for 45 minutes at 4°C in PBS/0.5% (w/v) BSA, together with FITC-labeled mouse antibodies against sca-1 and PE-labeled mouse antibodies against Flk-1 (BD Bioscience), or FITC-labeled mouse antibodies against CD34 (BD Bioscience), or PE-labeled mouse antibodies against CD11b (BD Bioscience). FACScan flow cytometry was performed and analyzed with Cell Quest software (BD Bioscience). To detect VE-cadherin, cells were incubated on ice with goat anti-mouse VE-cadherin (R&D Systems) for 20 minutes and then labeled with rabbit anti-goat Alexa Fluor 488 (R&D Systems) for 20 minutes. As staining control for both markers, 0.5% goat serum was used together with the identical secondary antibodies. Each analysis included at least 10,000 events.

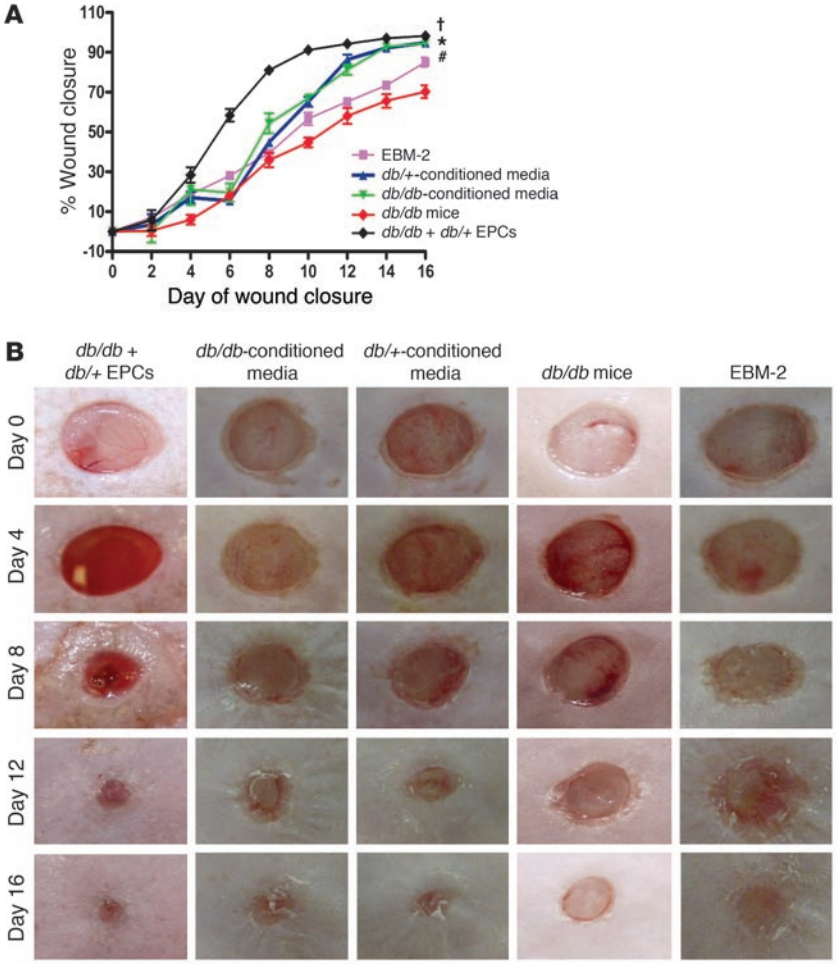

Figure 10
EPC-conditioned media on diabetic wound healing. Conditioned media collected from EPCs of *db*/+ and *db*/*db* mice were applied to the wounds of *db*/*db* mice every other day until day 16. EBM-2 was used as the control. The closure rate of 6-mm punch biopsies was measured every other day until day 16. (**A**) Conditioned media of *db*/+ EPCs and *db*/*db* EPCs similarly improved the rate of wound closure in diabetic mice, starting from day 10 (**P* < 0.05 vs. *db*/*db* mice treated with EBM-2; #*P*<0.05 vs. *db*/*db* mice only; *n* = 4). However, the overall rates of wound closure were significantly slower in *db*/*db* mice receiving conditioned media than those receiving normal EPC therapy (†*P* < 0.05 vs. *db*/*db* mice treated with *db*/+ EPCs, *n* = 4). (**B**) Typical photographs of wound healing.

Quantification of circulating EPCs. Mouse blood mononuclear cells were placed in polypropylene tubes in 100 μl PBS with 1% albumin. They were then stained with FITC-conjugated Sca-1 and PE-conjugated Flk-1 for 1 hour at 4°C and washed 3 times in PBS with 1% albumin (10). Quantification of Sca-1/Flk-1 double-positive cells was performed with a BD Vantage Flow cytometer.

Detection of ROS in EPCs. Blood mononuclear cells were placed in polypropylene tubes containing 5 μmol/l DHE (Invitrogen) in 100 μl PBS. Cells were incubated at 37°C for 10 minutes in a dark humidified chamber, washed 3 times in PBS, stained with Flk-1 and Sca-1 (BD Bioscience) for 1 hour at 4°C, and washed 3 times in PBS with 1% albumin. Quantification of DHE/Sca-1/Flk-1–positive cells was performed with a BD Vantage Flow cytometer. For mitochondrial superoxide detection, bone marrow–derived EPCs cultured with high glucose (25 mM) in EGM-2 were incubated with 5 μM MitoSOX (Invitrogen) for 20 minutes at 37°C, 5% CO_2. Cells were collected by trypsinization and washed 3 times with 1% albumin HBSS (with Ca/Mg), and mean fluorescent intensity was measured using flow cytometry (BD LSRII).

Western blot analysis of MnSOD. MnSOD protein was determined as we previously described (15). Briefly, EPCs were lysed in Cell Lytic MT lysis buffer (Sigma-Aldrich) with Protease Inhibitor Cocktail (100 μl Protease Inhibitor/10 ml lysis buffer; Sigma-Aldrich). Fifty μg of protein was separated on a 10% SDS-polyacrylamide gel, electrotransferred to nitrocellulose membranes (Bio-Rad), and incubated with a primary antibody against MnSOD (1:1,000; BD Transduction Laboratories) and the loading control anti-actin (1:1,000; Santa Cruz Biotechnology Inc.). The secondary antibodies were IRDye800–conjugated anti-mouse antibodies (1:4,000; Rockland). The blot was read with an Odyssey imager (Li-Cor), and molecular band intensity was determined with Odyssey 2.1 software (Li-Cor).

Real-time PCR for MnSOD, CuZnSOD, and catalase. EPCs were lysed and RNA was isolated with TRIzol (Invitrogen). For each sample, 2 μg RNA (measured with a NanoDrop ND-100) was reverse transcribed using SuperScript II RT, Oligo(dT) (Invitrogen) and dNTP Mix (Promega), with a GeneAmp PCR System 9700 (PE Applied Biosystems). Real-time PCR was carried out using SYBR Green PCR Master Mix on a 7500 Real-Time PCR System (Applied Biosystems). The primer sequences are as follows: MnSOD, forward 5′-CACATTAACGCGCAGATCATG-3′, reverse 5′-CCAGAGCCTCGTGGTACTTCTC-3′; CuZnSOD, forward 5′-ACCAGTGCAGGACCTCATTTTAA-3′, reverse 5′-TCTCCAACATGCCTCTCTTCATC-3′; catalase, forward 5′-ATGGCTTTTGACCCAAGCAA-3′, reverse 5′-CGGCCCTGAAGCTTTTTGT-3′; and 18S forward 5′-CGGGTCGGGAGTGGGT-3′, reverse 5′-GAAACGGCTACCACATCCAAG-3′. Variation in transcription levels was calculated using $2^{\Delta CT}$ (7).

MnSOD gene transfer of EPCs. Ex vivo gene transfer studies were conducted as described previously (40), with minor modifications. Briefly, replication-incompetent adenoviral vectors, driven by a cytomegalovirus promoter, were used to deliver MnSOD (Ad-MnSOD) or GFP marker gene (Ad-GFP) to the expanded EPCs in culture (500 multiplicity of infection) for 24 hours. EPCs were used 72 hours after the initial transfection.

MnSOD knockdown by siRNA in EPCs. After 7-day culture, EPCs were reseeded into 6-well plates at 2.5 × 10^5 cells/well. After 24 hours, the

MnSOD-siRNA SMARTpool (si-MnSOD, Dharmacon) was diluted to a 2 μM working solution and delivered to cells at 100 nM final concentration for 72 hours through a lipid-mediated DharmaFECT Transfection Reagent (Dharmacon). A non-related scramble siRNA (Dharmacon) was used as a transfection control.

EPC tube formation and adhesion assays. For tube formation assay, 24-well plates were coated with growth factor-reduced Matrigel (250 μl, Becton Dickinson). After 7 days in culture, bone marrow–derived EPCs (7.5×10^4) were plated in 500 μl EGM-2 medium and incubated at 37°C with 5% CO_2 for 24 hours. Tube formation was counted in 15 random fields, under ×100 magnification, with a Nikon Eclipse TE2000-U (23). For adhesion assay, 96-well plates were coated with 2.5 μg/ml rat vitronectin (Sigma-Aldrich) for 2 hours at 37°C. EPCs were plated at 1×10^4 cells/well in triplicate. After 2 hours of incubation at 37°C with 5% CO_2 in EGM-2, nonadherent cells were removed by washing 3 times with PBS. Cells were fixed with 2% paraformaldehyde and stained with Hoechst (Sigma-Aldrich). Five random fields were counted in each well under ×200 magnification.

Full-thickness excisional wounds. Punch biopsy wounds were created as previously described (7, 15). Briefly, mouse dorsum was clipped and depilatory cream (Nair) was used to remove hair. Skin was prepared with Betadine and allowed to dry. A full-thickness 6-mm skin punch biopsy (Acuderm) was created in each mouse. Wounds were dressed and changed every other day with a Bioclusive transparent oxygen permeable wound dressing (Johnson & Johnson). Wound closure rates were measured by tracing the wound area every other day onto an acetate paper. The tracings were digitized, and the areas were calculated by a computerized algorithm and converted to percent wound closure (Sigma-Aldrich Scan Pro 5, Jandel Scientific).

EPC therapy of diabetic wounds. For cell therapy of wounds, bone marrow–derived EPCs from *db/+* mice and AdMnSOD-transfected EPCs from *db/+* or *db/db* mice were trypsinized after 7 days in culture and resuspended in PBS. Then, 1×10^6 cells or 2×10^6 cells in 25 μl PBS were placed into the wound beds. A Bioclusive dressing was placed over the wound and mice remained under anesthesia for 15 minutes. Control mice were treated with PBS in the same fashion. Wound closure rates were compared between control and treatment groups, as we previously described (15).

Treatment of diabetic wounds with EPC-conditioned media. Bone marrow–derived mononuclear cells from diabetic and nondiabetic mice were plated on a vitronectin-coated (Sigma-Aldrich) 6-well plate at 8.5×10^5 cells/cm^2 in EGM-2 at 37°C with 5% CO_2. After 4 days of culture, nonadherent cells were removed and fresh EGM-2 was changed daily. At day 6 of culture, attached cells were washed once with endothelial basal medium-2 without growth factors and serum (EBM-2, Lonza) and incubated with EBM-2 (1 ml/well) for 24 hours (conditioned media). The conditioned media were then collected to treat diabetic wounds, and 25 μl conditioned media were injected onto and under the wound beds 0.5 cm past the wound edge every other day. Control mice were treated with PBS in the same fashion.

Wound angiogenesis. Wounds were recovered from mice on day 3, 6, and 16, as we previously described (15). Capillary density in the healing wounds was quantified by histological analysis. Wound samples were fixed with zinc chloride fixative (BD) for 24 hours, then embedded in paraffin, and sectioned at 4-μm intervals. Slides were deparaffinized and hydrated, then placed in Tris-Buffered Saline (pH 7.5) for 5 minutes for pH adjustment. Endogenous peroxidase was blocked by 3% Hydrogen Peroxide/Methanol bath for 20 minutes, followed by distilled H_2O rinses. Slides were blocked with normal rabbit serum (Vector Laboratories) for 30 minutes, then incubated for 60 minutes at room temperature with an anti-CD31 antibody (1:50; BD Bioscience), or an anti-vWF antibody (1:50; BD Bioscience), or an anti-CD34 antibody (1:50; BD Bioscience), and further incubated with Vectastain Elite ABC Reagent (Vector Laboratories) for 30 minutes and Nova Red (Vector Laboratories) for 15 minutes. Slides were counterstained with Gill (Lerner) 2 Hematoxylin (VWR Scientific) for 10 seconds, differentiated in 1% aqueous glacial acetic acid, and rinsed in running tap water. Ten random microscopic fields (×200 magnification) were counted to determine the number of capillaries per wound. Pictures were taken under a Nikon Eclipse TE2000-U microscope using Metamorph software.

In vivo EPC integration. On day 5 of culture, EPCs were labeled with 5-bromo-2′-deoxyuridine and 5-fluro-2′deoxyuridine (BrdU-labeling reagent, Invitrogen), as described previously (32, 40). Briefly, BrdU-labeling reagent was diluted to 1:100 in EGM-2, filtered through a 0.2-μm filter, and warmed to 37°C. One ml of BrdU/EGM-2 was added to cells in a 6-well plate, and new media were added daily until day 7. On day 7, the wells were washed 3 times with PBS, followed by trypsinization to resuspend the cells. As described above, 2×10^6 EPCs were then transplanted to a diabetic mouse wound (6-mm punch biopsy). After 6 days of wound healing, the mouse was euthanized, and the wound and surrounding skin was recovered and fixed in 10% formalin for 24 hours. Some slides were stained with an anti-BrdU antibody alone, and others were double-stained with an anti-CD31 antibody or an anti-vWF antibody, followed by BrdU antibody (1:50; Santa Cruz Biotechnology Inc.) incubation, as described above. Pictures were taken under a Nikon Eclipse TE2000-U microscope using Metamorph software.

Statistics. The results are presented as mean ± SEM. Pairwise comparisons were performed by a 2-tailed Student's *t* test, whereas multiple comparisons were tested with a 2-way ANOVA, followed by Bonferroni's correction to control type I error (41). The analysis for the rate of wound healing among groups was preformed by SAS (Version 9.1) mixed procedure, followed with Bonferroni's correction. In all the tests, a 2-tailed *P* value of less than 0.05 was taken as evidence of a statistically significant finding.

Acknowledgments

This work was funded by grant R01GM077352 from the National Institute of General Medical Science, NIH; grant 7-08-RA-23 from the American Diabetes Association; and International Collaborative grant 30728021 from the Natural Sciences Foundation of China (to A.F. Chen). E.J. Marrotte is a receipt of an American Heart Association predoctoral fellowship award (0615519Z), and D.D. Chen is a receipt of an American Heart Association postdoctoral fellowship award (0720114Z).

Received for publication July 16, 2010, and accepted in revised form September 8, 2010.

Address correspondence to: Alex F. Chen, VA Vascular Surgery Research, Department of Surgery, University of Pittsburgh School of Medicine, W1148 Biomedical Science Tower, 200 Lothrop Street, Pittsburgh, Pennsylvania 15213, USA. Phone: 412.624.6769; Fax: 412.648.7107; E-mail: chena5@upmc.edu.

1. Brem H, Sheehan P, Rosenberg HJ, Schneider JS, Boulton AJ. Evidence-based protocol for diabetic foot ulcers. *Plast Reconstr Surg*. 2006; 117(7 suppl):193S–209S.
2. Jeffcoate WJ, Harding KG. Diabetic foot ulcers. *Lancet*. 2003;361(9368):1545–1551.
3. Barcelos LS, et al. Human CD133+ progenitor cells promote the healing of diabetic ischemic ulcers by paracrine stimulation of angiogenesis and activation of Wnt signaling. *Circ Res*. 2009;104(9):1095–1102.
4. Roncalli JG, Tongers J, Renault MA, Losordo DW. Endothelial progenitor cells in regenerative medicine and cancer: a decade of research. *Trends Biotechnol*. 2008;26(5):276–283.
5. Loomans CJ, et al. Endothelial progenitor cell dysfunction: a novel concept in the pathogenesis of vascular complications of type 1 diabetes. *Diabetes*. 2004; 53(1):195–199.
6. Fadini GP, et al. Circulating endothelial progenitor cells are reduced in peripheral vascular complications of type 2 diabetes mellitus. *J Am Coll Cardiol*. 2005; 45(9):1449–1457.
7. Asai J, et al. Topical sonic hedgehog gene therapy accelerates wound healing in diabetes by enhancing

endothelial progenitor cell-mediated microvascular remodeling. *Circulation*. 2006;113(20):2413–2424.
8. Gallagher KA, et al. Diabetic impairments in NO-mediated endothelial progenitor cell mobilization and homing are reversed by hyperoxia and SDF-1 alpha. *J Clin Invest*. 2007;117(5):1249–1259.
9. Tepper OM, et al. Human endothelial progenitor cells from type II diabetics exhibit impaired proliferation, adhesion, and incorporation into vascular structures. *Circulation*. 2002;106(22):2781–2786.
10. Awad O, Jiao C, Ma N, Dunnwald M, Schatteman GC. Obese diabetic mouse environment differentially affects primitive and monocytic endothelial cell progenitors. *Stem Cells*. 2005;23(4):575–583.
11. Caballero S, et al. Ischemic vascular damage can be repaired by healthy, but not diabetic, endothelial progenitor cells. *Diabetes*. 2007;56(4):960–967.
12. Peppa M, Stavroulakis P, Raptis SA. Advanced glycoxidation products and impaired diabetic wound healing. *Wound Repair Regen*. 2009;17(4):461–472.
13. Brownlee M. Biochemistry and molecular cell biology of diabetic complications. *Nature*. 2001; 414(6865):813–820.
14. Rolo AP, Palmeira CM. Diabetes and mitochondrial function: role of hyperglycemia and oxidative stress. *Toxicol Appl Pharmacol*. 2006;212(2):167–178.
15. Luo JD, Wang YY, Fu WL, Wu J, Chen AF. Gene therapy of endothelial nitric oxide synthase and manganese superoxide dismutase restores delayed wound healing in type 1 diabetic mice. *Circulation*. 2004; 110(16):2484–2493.
16. Tie L, Li XJ, Wang X, Channon KM, Chen AF. Endothelium-specific GTP cyclohydrolase I overexpression accelerates refractory wound healing by suppressing oxidative stress in diabetes. *Am J Physiol Endocrinol Metab*. 2009;296(6):E1423–E1429.
17. He T, et al. Human endothelial progenitor cells tolerate oxidative stress due to intrinsically high expression of manganese superoxide dismutase. *Arterioscler Thromb Vasc Biol*. 2004;24(11):2021–2027.
18. Dernbach E, Urbich C, Brandes RP, Hofmann WK, Zeiher AM, Dimmeler S. Antioxidative stress-associated genes in circulating progenitor cells: evidence for enhanced resistance against oxidative stress. *Blood*. 2004;104(12):3591–3597.
19. Chen DD, Chen AF. CuZn superoxide dismutase deficiency: culprit of accelerated vascular aging process. *Hypertension*. 2006;48(6):1026–1028.
20. Krankel N, et al. Hyperglycemia reduces survival and impairs function of circulating blood-derived progenitor cells. *Arterioscler Thromb Vasc Biol*. 2005; 25(4):698–703.
21. Balestrieri ML, et al. High glucose downregulates endothelial progenitor cell number via SIRT1. *Biochim Biophys Acta*. 2008;1784(6):936–945.
22. Feng Y, et al. Critical role of scavenger receptor-BI-expressing bone marrow-derived endothelial progenitor cells in the attenuation of allograft vasculopathy after human apo A-I transfer. *Blood*. 2009; 113(3):755–764.
23. Zhao T, Li J, Chen AF. MicroRNA-34a induces endothelial progenitor cell senescence and impedes its angiogenesis via suppressing silent information regulator 1. *Am J Physiol Endocrinol Metab*. 2010; 299(1):E110–E116.
24. Miller G, Honig A, Stein H, Suzuki N, Mittler R, Zilberstein A. Unraveling delta1-pyrroline-5-carboxylate (P5C)/proline cycle in plants by uncoupled expression of proline oxidation enzymes. *J Biol Chem*. 2009;284(39):26482–26492.
25. Sasaki M, Abe R, Fujita Y, Ando S, Inokuma D, Shimizu H. Mesenchymal stem cells are recruited into wounded skin and contribute to wound repair by transdifferentiation into multiple skin cell type. *J Immunol*. 2008;180(4):2581–2587.
26. Suh W, et al. Transplantation of endothelial progenitor cells accelerates dermal wound healing with increased recruitment of monocytes/macrophages and neovascularization. *Stem Cells*. 2005; 23(10):1571–1578.
27. Luo JD, Hu TP, Wang L, Chen MS, Liu SM, Chen AF. Sonic hedgehog improves delayed wound healing via enhancing cutaneous nitric oxide function in diabetes. *Am J Physiol Endocrinol Metab*. 2009; 297(2):E525–E531.
28. Jimenez-Quevedo P, et al. Diabetic and nondiabetic patients respond differently to transendocardial injection of bone marrow mononuclear cells: findings from prospective clinical trials in "no-option" patients. *Rev Esp Cardiol*. 2008;61(6):635–639.
29. Niu Y, Epperly MW, Shen H, Smith T, Wang H, Greenberger JS. Intraesophageal MnSOD-plasmid liposome enhances engraftment and self-renewal of bone marrow derived progenitors of esophageal squamous epithelium. *Gene Ther*. 2008;15(5):347–356.
30. Case J, Ingram DA, Haneline LS. Oxidative stress impairs endothelial progenitor cell function. *Antioxid Redox Signal*. 2008;10(11):1895–1907.
31. Krenning G, van Luyn MJ, Harmsen MC. Endothelial progenitor cell-based neovascularization: implications for therapy. *Trends Mol Med*. 2009; 15(4):180–189.
32. Dubois C, et al. Differential effects of progenitor cell populations on left ventricular remodeling and myocardial neovascularization after myocardial infarction. *J Am Coll Cardiol*. 2010;55(20):2232–2243.
33. Mantzoros CS, Moschos SJ. Leptin: in search of role(s) in human physiology and pathophysiology. *Clin Endocrinol (Oxf)*. 1998;49(5):551–567.
34. Schafer K, et al. Leptin promotes vascular remodeling and neointimal growth in mice. *Arterioscler Thromb Vasc Biol*. 2004;24(1):112–117.
35. Wolk R, Deb A, Caplice NM, Somers VK. Leptin receptor and functional effects of leptin in human endothelial progenitor cells. *Atherosclerosis*. 2005; 183(1):131–139.
36. Galiano RD, et al. Topical vascular endothelial growth factor accelerates diabetic wound healing through increased angiogenesis and by mobilizing and recruiting bone marrow-derived cells. *Am J Pathol*. 2004;164(6):1935–1947.
37. Tsuboi R, Shi CM, Rifkin DB, Ogawa H. A wound healing model using healing-impaired diabetic mice. *J Dermatol*. 1992;19(11):673–675.
38. Ingram DA, et al. In vitro hyperglycemia or a diabetic intrauterine environment reduces neonatal endothelial colony-forming cell numbers and function. *Diabetes*. 2008;57(3):724–731.
39. Thum T, et al. Endothelial nitric oxide synthase uncoupling impairs endothelial progenitor cell mobilization and function in diabetes. *Diabetes*. 2007; 56(3):666–674.
40. Iwaguro H, et al. Endothelial progenitor cell vascular endothelial growth factor gene transfer for vascular regeneration. *Circulation*. 2002;105(6):732–738.
41. Ludbrook J. Repeated measurements and multiple comparisons in cardiovascular research. *Cardiovasc Res*. 1994;28(3):303–311.